Engineering Notes

ENGINEERING NOTES are short manuscripts describing new developments or important results of a preliminary nature. These Notes cannot exceed 6 manuscript pages and 3 figures; a page of text may be substituted for a figure and vice versa. After informal review by the editors, they may be published within a few months of the date of receipt. Style requirements are the same as for regular contributions (see inside back cover).

Heating Distributions for a 0.006-Scale Shuttle Orbiter over a Range of Hypersonic Flow Conditions

Charles G. Miller*
NASA Langley Research Center, Hampton, Virginia

Introduction

THE effect of Reynolds number on hypersonic flowfield characteristics may be studied experimentally in most hypersonic, conventional-type wind tunnels by varying reservoir conditions. However, the study of Mach number effects and gamma effects requires the use of several tunnels. Generally, this involves different data reduction procedures (particularly in the study of gamma effects) and often different models to study the effect of these three flow quantities, thereby introducing additional uncertainties. The hypersonic heat-transfer data base for the Space Shuttle Orbiter, derived primarily from ideal-air wind tunnel tests, is an example of this multitunnel, multimodel approach. To the author's knowledge, the open literature is free of a systematic study to determine the effect of Reynolds number, Mach number, and gamma on heating to a single Orbiter model and with the same data reduction procedure. For this reason, and to add to the existing heat-transfer data base, a study was performed in which heating distributions were measured on a 0.006-scale Orbiter model (147B lines) over a range of hypersonic conditions.[1] Three wind tunnels were used in this study: the Langley 20-in. Mach 6 Tunnel, Continuous Flow Hypersonic Tunnel, and Hypersonic CF_4 Tunnel, thus providing a variation in Mach number from 6 to 10 in air, range of Reynolds number at Mach 6 and 10, and variation in gamma from 1.13 to 1.4 at Mach 6. This variation in gamma is particularly noteworthy since it causes a change in shock detachment distance and shock inclination which in turn influences conditions along the outer edge of the boundary layer, hence heat transfer. Thus, the CF_4 data provide qualitative information on the effect of a decrease in gamma within the flowfield, such as occurs for real-air in thermochemical equilibrium. To insure meaningful comparisons between these facilities, especially between air and CF_4, Orbiter heating rates were nondimensionalized by the stagnation-point heat transfer to a sphere measured in each facility at the same flow conditions as the Orbiter. The purpose of this Note is to present a sample of these experimental results, in the form of windward-centerline heating distributions, over a wide range of angle of attack and compare prediction to experiment.

Apparatus and Tests

Descriptions of the Langley 20-in. Mach 6 Tunnel, Continuous Flow Hypersonic Tunnel, and Hypersonic CF_4 Tunnel, along with calibration results, are presented in Refs. 2, 3, and 4, respectively.

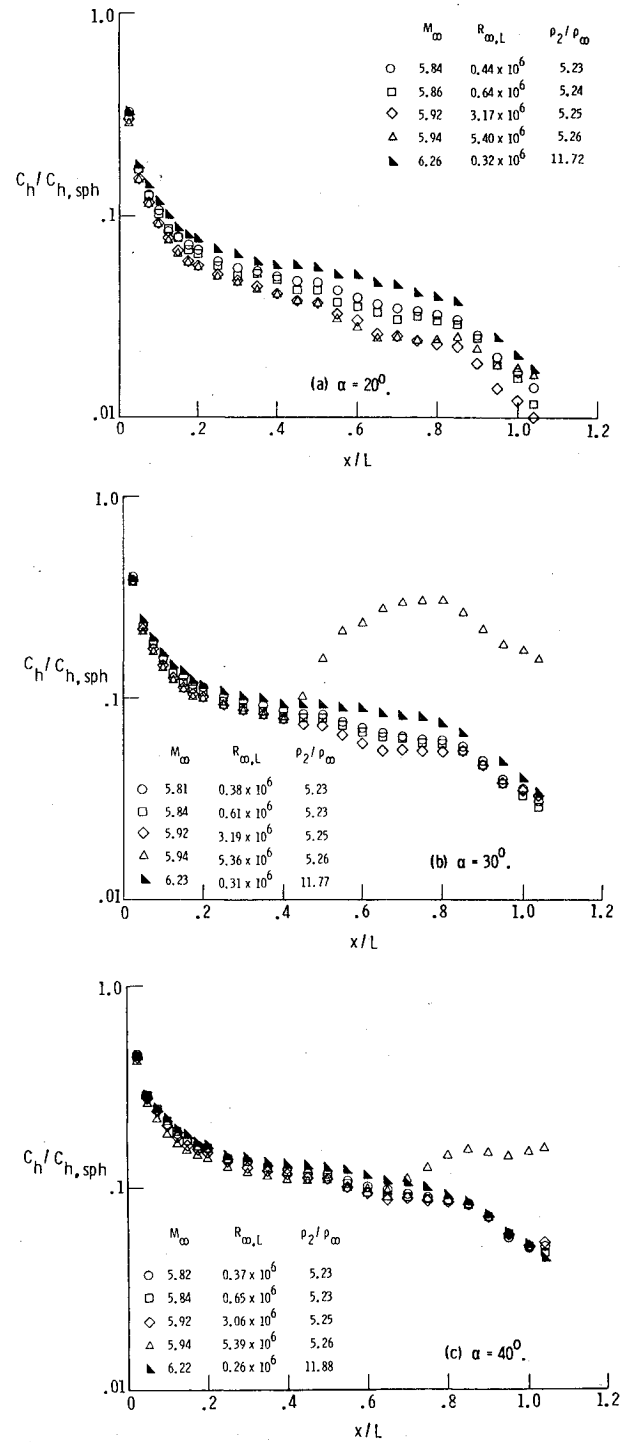

Fig. 1 Windward-centerline heating distributions at various angles of attack in Mach 6 air and CF_4.

Presented as Paper 82-0826 at the AIAA/ASME Third Joint Thermophysics Fluids, Plasma and Heat Transfer Conference, St. Louis, Mo., June 7-11, 1982; submitted Jan. 31, 1983; revision received April 3, 1983. This paper is declared a work of the U.S. Government and therefore is in the public domain.

*Aero-Space Engineer, Aerothermodynamics Branch, Space Systems Division. Member AIAA.

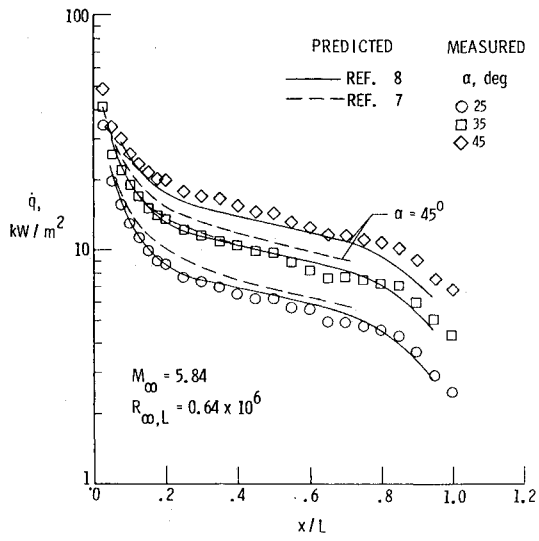

Fig. 2 Measured and predicted windward-centerline laminar heating distributions in air.

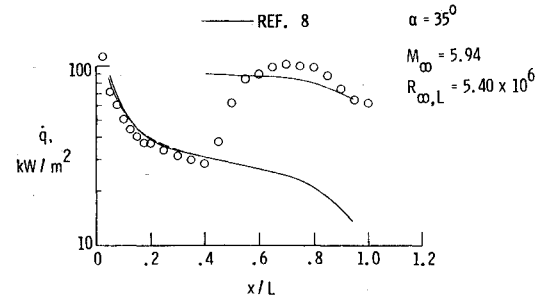

Fig. 3 Measured and predicted windward-centerline transitional heating distributions in air.

The 0.006-scale Shuttle Orbiter model (designated as model 50-0)[5] contains 89 iron-constantan thermocouples spot-welded to the inner surface of inserts machined flush with the model surface. Body flap and elevon deflections are fixed at 0 deg. Values of Reynolds number are based on the measured length L of the model from nose tip to body flap hinge line, which is 19.6 cm. A 10.16 cm diam, continuous thin-skin sphere was also tested in the three facilities at the same flow conditions as the Orbiter model. Angle of attack for the Orbiter model was varied from 5 to 45 deg in 5 deg increments, and the yaw angle was zero.

Heat-transfer rates to the continuous thin-skin sphere and Orbiter thin-skin inserts were calculated using the one-dimensional, transient, calorimeter equation.[1,6] Results are presented in terms of the measured heat-transfer rate $\dot{q}$ and to reduce the influence of wall temperature ratio between the various wind tunnels, as the ratio of heat-transfer coefficient for the Orbiter to that for the sphere, $C_h/C_{h,\mathrm{sph}}$. The heat-transfer coefficient is defined in terms of the total temperature $T_{t,2}$ and the outer-surface temperature or wall temperature T_w, $C_h = \dot{q}/(T_{t,2} - T_w)$. The full-scale sphere radius used to determine $C_{h,\mathrm{sph}}$ was 0.7 m instead of the usual reference value of 0.3 m. This value of 0.7 m is the approximate equivalent Orbiter nose radius and for a 0.006 scale is equal to 0.419 cm. More details of the facilities, models, instrumentation, test conditions, data reduction, and uncertainties are provided in Ref. 1.

Prediction

Heating distributions along the windward centerline were predicted using two methods.[7,8] The method of Zoby[7] employs a rapid, inviscid-flowfield procedure coupled with laminar and turbulent heating equations which can be computed for constant or variable-entropy edge conditions. An equivalent axisymmetric body (hyperboloid) is used to model the coordinates of the Orbiter windward-symmetry plane at angles of attack. The method of Hamilton[8] is based on a "local infinite-swept cylinder" analysis and includes an approximation for entropy swallowing. Both laminar and turbulent heating rates are generated.

Results

The laminar ratio of heat-transfer coefficients $C_h/C_{h,\mathrm{sph}}$ for Mach 6 air increased with decreasing Reynolds number (Fig. 1). This effect of Reynolds number decreases with increasing angle of attack α, corresponding to an effective blunter body and decreasing viscous effects, and is within the experimental uncertainty in heat-transfer rate for $\alpha \geq 35$ deg. A decrease in $C_h/C_{h,sph}$ with increasing $R_{\infty,L}$ has been observed at Mach 8 in air[9] for $\alpha = 20$ deg, but this ratio was essentially independent of $R_{\infty,L}$ for 25 deg $\leq \alpha \leq$ 45 deg. The results of Fig. 1 indicate the effect of Reynolds number on centerline heating during the hypersonic, high-altitude portion of early Orbiter re-entries, where $\alpha > 30$ deg, will be small. However, as the crossrange is increased in future flights, corresponding to lower α, Reynolds number effects on centerline heating may become significant.

The ratio $C_h/C_{h,\mathrm{sph}}$ was observed to be independent of Mach number between 6 and 10 in air for a given Reynolds number and $\alpha \geq 15$ deg. For $\alpha \leq 10$ deg, $C_h/C_{h,\mathrm{sph}}$ increased with decreasing Mach number, typical of relatively slender, spherically blunted cones.[10]

An increase in the ratio of heat-transfer coefficients along the windward centerline with decreasing gamma (increasing density ratio) at the lower angles of attack is implied in Fig. 1. Although the small difference in Mach number between air and CF_4 and the lower $T_w/T_{t,2}$ for CF_4 should not significantly influence $C_h/C_{h,\mathrm{sph}}$ for the range of α shown in Fig. 1, the difference in Reynolds number may. Because of a low supply of CF_4, only a few runs were possible in the CF_4 tunnel at higher reservoir pressures to match the Reynolds number in air ($R_{\infty,L} \approx 0.4 \times 10^6$). These runs verified the existence of a gamma effect on Orbiter heating. Thus, the present results imply higher equilibrium heating rates would be experienced in high cross-range flight than inferred from tests in ideal-air flow.

Laminar heating distributions in Mach 6 air were accurately (within 10% for $0.1 < x/L < 0.8$) predicted by the local infinite-swept cylinder analysis[8] for 25 deg $\leq \alpha \leq$ 45 deg. (Fig. 2). The method of Zoby[7] was also quite accurate for $\alpha = 35$ and 40 deg but underpredicted $\dot{q}$ at $\alpha = 45$ deg and overpredicted $\dot{q}$ at $\alpha = 25$ deg. Relations for the thermodynamic and transport properties for CF_4 were incorporated into the method of Zoby and an increase in heating with decreasing gamma was predicted at $\alpha = 35$ deg, agreeing with the measured trend.[1] Boundary-layer transition occurred along the windward centerline at the highest Reynolds number in Mach 6 air (Figs. 1 and 3). The swept-cylinder method[8] provides a reasonable prediction of fully turbulent heating as observed in Fig. 3.

In summary, the effects of Mach number, Reynolds number, and gamma on centerline heating are essentially negligible for the angle-of-attack range corresponding to the hypersonic portion of early Orbiter flights. As the crossrange is increased in future flights, corresponding to lower angles of attack, the effect of each of these three flow quantities on heating may become significant.

References

[1] Miller, C.G., "Experimental Investigation of Gamma Effects on Heat Transfer to a 0.006-Scale Shuttle Orbiter at Mach 6," AIAA Paper 82-0826, June 1982.

[2] Miller, C.G. III and Gnoffo, P.A., "Pressure Distributions and Shock Shapes for 12.84°/7° On-Axis and Bent-Nose Biconics in Air at Mach 6," NASA TM 83222, 1981.

[3]Miller, C.G., "Measured Pressure Distributions, Aerodynamic Coefficients and Shock Shapes on Blunt Bodies of Revolution at Incidence in Mach 6 Air and CF_4 and Mach 10 Air," NASA TM 84489, Sept. 1982.

[4]Midden, R.E. and Miller, C.G., "Description and Preliminary Calibration Results for the Langley Hypersonic CF_4 Tunnel," NASA TM 78800, 1978.

[5]Foust, J.W., "Entry Heat Transfer Tests of the 0.006-Scale Space Shuttle (−147B) Orbiter Model (50-0) in the Langley Research Center Freon Tunnel at Mach 6 (OH45)," NASA CR-141,527, Dec. 1975.

[6]Miller, C.G. III, "Comparison of Thin-Film Resistance Heat-Transfer Gages with Thin-Skin Transient Calorimeter Gages in Conventional Hypersonic Wind Tunnels," NASA TM 83197, Dec. 1981.

[7]Zoby, E.V., "Approximate Heating Analysis for the Windward-Symmetry Plane of Shuttle-Like Bodies at Large Angle of Attack," *Thermophysics of Atmospheric Entry: AIAA Progress in Astronautics and Aeronautics,* Vol. 82, edited by T.E. Horton, AIAA, New York, 1982, pp. 229-247.

[8]Hamilton, H.H., "Approximate Method of Predicting Heating on the Windward Side of Space Shuttle Orbiter and Comparisons with Flight Data," AIAA Paper 82-0823, June 1982.

[9]Herrera, B.J., "Results From a Convective Heat Transfer Rate Distribution Test on a 0.0175 Scale Model (22-0) of the Rockwell International Vehicle 4 Space Shuttle Configuration in the AEDC-VKF Tunnel B (OH498)," Vol. 1 of 2, NASA CR-147,626, 1976.

[10]Griffith, B.J., Majors, B.M., and Adams, J.C., "Blunt Body Boundary-Layer Parameters Including Shock Swallowing Effects," *Thermophysics of Atmospheric Entry: AIAA Progress in Astronautics and Aeronautics,* Vol. 82, edited by T.E. Horton, AIAA, New York, 1982, pp. 90-111.

A Novel Concept for Reducing Thermal Contact Resistance

R.S. Cook,* K.H. Token,† and R.L. Calkins‡
McDonnell Aircraft Company,
St. Louis, Missouri

Introduction

MECHANICAL joints, which must be opened periodically for equipment inspection or maintenance, are encountered in many equipment cooling designs, particularly those for electronic equipment. The thermal contact resistance at interfaces in electronics either elevates operating temperatures, which degrades component reliability, or increases coolant demand, which increases cooling system size and power requirements.

A novel concept for reducing thermal contact resistance has been identified and tested. It does not require high contact pressure or smooth surface finishes for good thermal performance, and it does not inhibit joint assembly or disassembly.

The Improved Thermal Joint Concept

The key feature of this new concept is the incorporation of a low-melting-point metallic alloy in an interstitial material. At room temperature the alloy is in the solid state to aid assembly and disassembly of the joint. The selected alloy has a melting point below the operating temperature of the joint. During operation, heat transferred to the joint raises the interface temperature, causing the alloy to change phase to the liquid state. The liquid metal then flows freely to fill the interstitial voids, as indicated in Fig. 1.

The improved thermal joint has several noteworthy characteristics. When the alloy is liquid it provides a continuous metallic heat-transfer path, which significantly reduces contact resistance. Since the alloy is liquid at operating temperatures, high contact pressure is not required to force the interstitial material into voids. Joint disassembly after cool down and solidification of the alloy is accomplished easily since many low-melting-point alloys will not adhere strongly to metallic or nonmetallic surfaces unless they are exceptionally clean and free of oxides. Also, a number of candidate alloys are available (see Ref. 1 for a list of 190 alloys with melting points ranging from −54 to 590°F).

Improved Thermal Joint Embodiments

Three embodiments have been investigated. The first (Fig. 2) employs a porous metallic structure (carrier) to contain the liquid metal alloy. Capillarity prevents the liquid metal from flowing out of the interstice during inertial or gravitational accelerations. This embodiment is referred to as the "porous carrier."

The second embodiment (Fig. 2) consists of a thin sheet of solid carrier material (e.g., copper or copper-plated aluminum) coated on both sides with a thin layer of the low-melting-point alloy, which is inserted between the joining surfaces. At operating temperature the alloy liquifies and fills the interstitial voids. Following cool down and solidification, the alloy is retained on the carrier by a strong bond. The bond with the surface material is weak, however, allowing easy separation of the joint and removal of the alloy-coated carrier. This embodiment is referred to as the "solid carrier." For those applications where a separable carrier is undesirable, the carrier material (e.g., electroplated copper) can be applied directly to one of the joining surfaces.

The third embodiment (Fig. 2) consists of a thin sheet of low-melting-point alloy which is inserted between the joining surfaces. When heated, the alloy liquifies and fills the interstitial voids. The weak affinity between the alloy and the surface material allows easy separation of the cold joint. Thermal performance is restored by inserting a new sheet of alloy between the joining surfaces during reassembly. This embodiment is referred to as the "alloy" joint.

Development Test Program

A test program was conducted to verify the improved thermal joint concept and develop the most promising embodiment. Preliminary tests established approximate thermal contact resistance values for each embodiment in contact with 6061-T6 aluminum surfaces, frequently encountered in electronic packaging. Static measurements based on the thermal comparator method indicated significantly less contact resistance than for a reference bare aluminum joint. Prototypes were accelerated on a centrifuge to evaluate each for loss of liquid metal from the interstice. Additional static

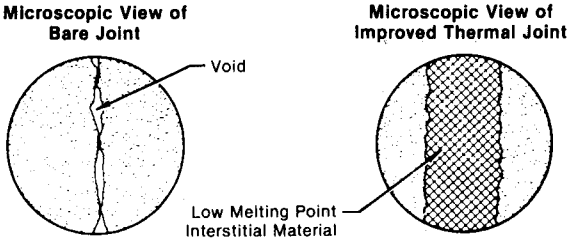

Fig. 1 Improved thermal joint concept.

Presented as Paper 82-0886 at the AIAA/ASME 3rd Joint Thermophysics, Fluids, Plasma and Heat Transfer Conference, St. Louis, Mo., June 7-11, 1982; submitted June 14, 1982; revision received March 31, 1983.

*Technical Specialist, Propulsion and Thermodynamics Department, Engineering Technology Division.

†Branch Chief, Propulsion and Thermodynamics Department, Engineering Technology Division. Member AIAA.

‡Senior Engineer, Materials Laboratory, Flight and Laboratory Development Division.